Michelson Interferometer Design for Linac Coherent Light Source (LCLS) Applications in the 15 -1.5 Å Wavelength Range

Roman Tatchyn[a]

Stanford Synchrotron Radiation Laboratory, Stanford Linear Accelerator Center, Stanford, CA 94305, USA
[a]*Corresp. Author: Ph: (650) 926-2731; FAX: (650) 926-4100; e-mail: tatchyn@ssrl.slac.stanford.edu*

Abstract. In recent years the continuing development of linac-driven X-Ray Free Electron Laser (XRFEL) designs has significantly expanded the parameter space associated with 3rd and earlier-generation synchrotron radiation sources. In particular, in contrast to the > 100 ps pulse durations typical of storage rings, temporal lengths extending down to the <100 fs regime will become available. For example, for the SLAC Linac Coherent Light Source (LCLS) a pulse duration of ~ 200-300 fs with finer temporal features extending down to ~1 fs is anticipated. The characterization of the phase space distributions of such pulses poses a significant challenge for instrumentation design both with regard to the brevity of the pulse structure as well as the X-ray (15-1.5 Å) wavelength range of the FEL line. In this paper we assess a Michelson interferometer design aimed at characterizing the coherence length of the SLAC LCLS and discuss considerations related to its operation.

1. INTRODUCTION

Time-domain autocorrelation can be used to obtain information on the power spectral density of a temporal signal. In particular, it can provide information on the temporal coherence length of a quasi-coherent source (1). In the case of the LCLS, this is a critically important parameter directly related to the FEL-induced microbunch structure in the electron beam (2), and provisions for characterizing its statistics are presently under study by the LCLS X-Ray Optics R&D group (3). In this paper we describe the design of a novel type of Michelson X-ray interferometer matched to the phase space parameters of the SLAC LCLS. In the subsequent section a brief review of LCLS source properties critical to the design of the instrument is given, and in the following sections the layout and operating principles of the interferometer are described.

2. SOURCE PARAMETERS OF THE SLAC LCLS

As is known, the LCLS pulse phase space parameters extend into X-ray regimes in which very little experience has been acquired (4). To illustrate, a set of typical source parameters are listed in Table 1 and a graphical display of the temporal and spectral profiles of a representative LCLS SASE pulse is shown in Fig. 1. It is evident that, in contrast to a storage ring source, the LCLS pulse (in the lab frame) can be roughly characterized as having an aspect ratio of ~ 1 in all three planes. Furthermore, it can be viewed as being constituted of a random longitudinal distribution of flat "sheets" of radiation of average sub-femtosecond thickness and an order-of-magnitude variation in intensity, each with a large transverse:longitudinal (O(~100)) aspect ratio.

TABLE 1. LCLS radiation pulse parameters. Undulator K=3.67. N_u=3300 periods. Undulator period λ_u=3 cm.

Radiation wavelength [Å]	**1.5**	**15**
Bunch duration [fs, FWHM]	**277**	**277**
Coherent photons/pulse (x10^{12})	**1.9**	**23**
Approx. Bandwidth (BW) [%]	**0.1**	**0.1**
Transverse size [μm, FWHM]*	**78**	**93**
Divergence angle [μrad, FWHM]*	**1**	**8**

*At undulator exit

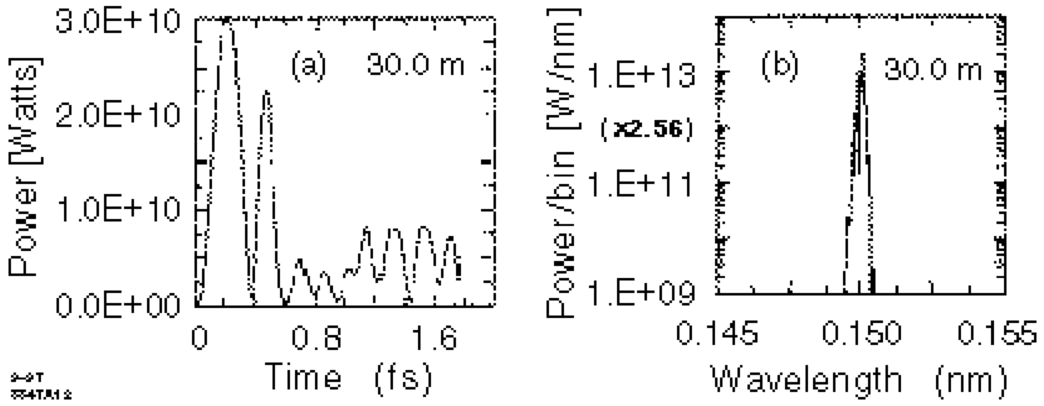

Figure 1. Temporal (a))and spectral (b)) features of the saturated output of a 30 m 1.5 Å SASE FEL. The abscissa of b) is divided into 256 bins.

An overview of the general consequences of these properties on the design of optical instrumentation in the X-ray range has been presented elsewhere (5). With regard to interferometer design, a basic requirement is to minimize distortions in the temporal structure of the pulse so that valid autocorrelation spectra can be generated. To achieve this, it can be shown that optical elements with sufficiently weak angular and spectral dispersion in the spectral range of interest need to be employed. A second requirement, arising from the extreme power density of the LCLS pulses (see Table 1), is that the response of an optical element interacting with an LCLS pulse should remain sufficiently uninfluenced by the energy being absorbed during the interaction. For the interferometer under discussion, these requirements are critical to the design and mode of operation of the beam splitting mechanism, as well as in the optimization of the parameters and geometry of the reflecting elements.

3. ASYMMETRIC MICHELSON INTERFEROMETER

A schematic of the proposed instrument is shown in Fig. 2. Although a transmission grating splitter is explicitly shown, techniques based on reflecting/transmitting foils (6) could also be considered. The split beams are reflected off mirrors M1 and M2 and recombine at the detector plane. With the mirrors parallel the path length difference between the two interferometer arms is 0. To induce a path length difference M1 is rotated counterclockwise through an angle Δθ. At the same time, the detector is rotated through the same angle and translated back a distance r_2.

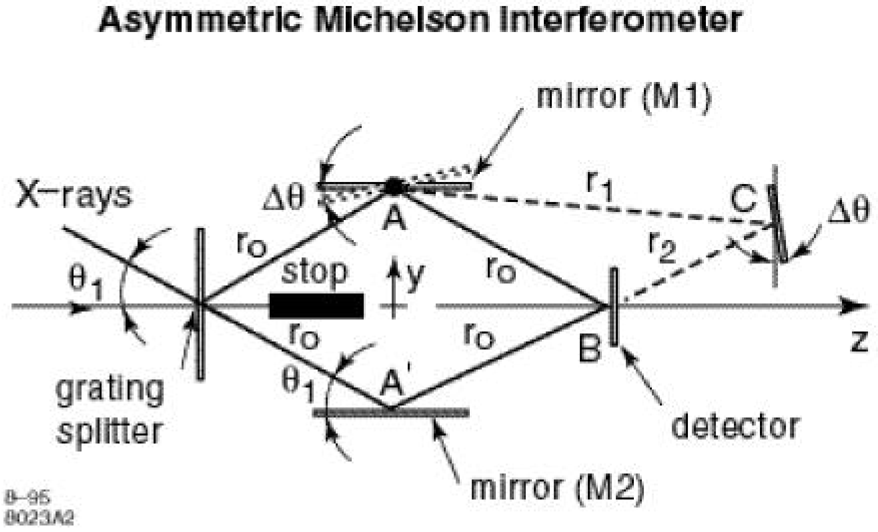

FIGURE 2. Schematic layout of an asymmetric Michelson autocorrelator based on a grating splitter.

As Δθ is tuned, the path difference Δr between the two arms is given by

$$\Delta r = (r_0 + r_2) - r_1 = 2r_0 \cdot \left\{ \frac{\sin(q_1)\sec(q_1 - 2\Delta q) - \tan(q_1)}{\tan(q_1) + \tan(q_1 - 2\Delta q)} \right\} \tag{1}$$

and the stroke distance r_2 of the scanning/rotating detector by

$$r_2 = r_0 \cdot \left\{ \frac{\tan(q_1) - \tan(q_1 - 2\Delta q)}{\tan(q_1) + \tan(q_1 - 2\Delta q)} \right\} . \tag{2}$$

To illustrate parameter dependence, expand Δr about Δθ=0 . This yields:

$$\Delta r \cong (2 r_0 q_1)\, \Delta q - (2 r_0 q_1{}^2)\, \Delta q^2 + \ldots \tag{3}$$

and

$$r_2 \cong r_0 \cdot \left(\frac{\Delta q}{(q_1 - \Delta q)} \left\{ 1 + \frac{2}{3} q_1{}^2 \right\} - \frac{4 q_1}{3} \frac{\Delta q^2}{(q_1 - \Delta q)} + \ldots \right) \quad . \tag{4}$$

To illustrate a typical parameter range, let r_0=0.5m. In Fig. 3 the variables r_2 and Δr are plotted as functions of Δθ for two values of θ_1.

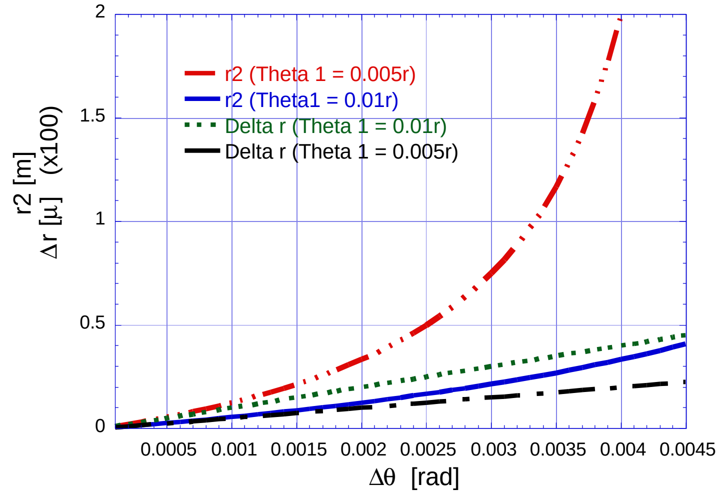

FIGURE 3. Tuning curves for an asymmetric Michelson autocorrelator for two different starting values of θ_1. r_0=0.5m. The ordinate values for each curve scale linearly with r_0.

For a given starting value of θ_1 (viz., in the symmetric limit), the reflectivities of M1 and M2 are equal. As the device is tuned, the reflectivity of M1 will increase (assuming it is a specular reflector), inducing an asymmetric scaling in the relative amplitudes of the interferometer beams. In this regard, the maximal asymmetry, as well as the maximum power loading condition, for specular interferometer facets will be determined by the mirror material and θ_1. To illustrate the range of Z-dependent reflectivities accessible with specular mirror materials curves spanning the 1 keV - 8.5 keV range of the LCLS fundamental are plotted vs. θ_1 for gold and beryllium (7) in Fig. 4. Corresponding to these curves, the energy loading η[eV/atom] induced in the mirror material - assuming irradiation with the full unattenuated LCLS beam (8) - is plotted in Fig. 5. It is evident that in order to develop a value of Δr of the same order of length as the LCLS pulse without excessive values of r_0 or r_2 the preferred value of θ_1 will lie in the > 0.005 rad range. In order to operate in this range, it consequently follows that substantial attenuation of the LCLS beam will be desirable prior to reflection in the interferometer. In the present design this can be accomplished in part by the grating splitter, whose diffraction efficiency can be controlled by adjusting the parameters (primarily the thickness) of the transmission grating. Without upstream attenuation the grating itself is likely to be damaged; however, a new grating, or grating area, could be inserted between shots, which would also allow for spectral tuning. The basic requirements on the grating parameters is that the dispersion be small enough to preserve the temporal structure of the LCLS pulses and that the spectral bandwidth of the diffracted orders be substantially larger than the bandwidth of the LCLS radiation.

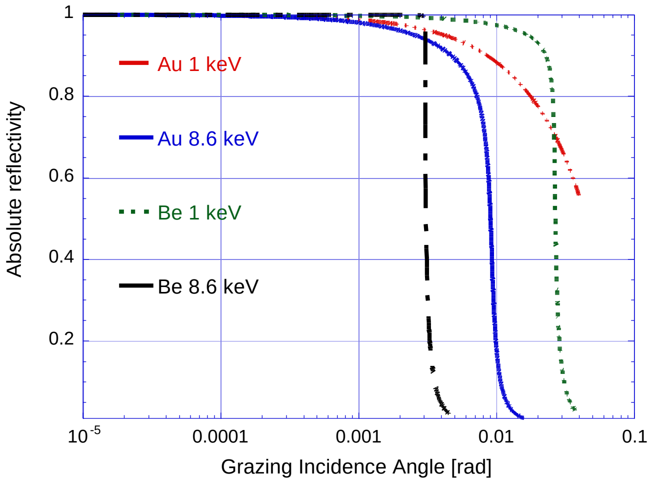

FIGURE 4. Absolute reflectivities of Au and Be vs. grazing incidence angle at photon energies of 1 and 8.6 keV.

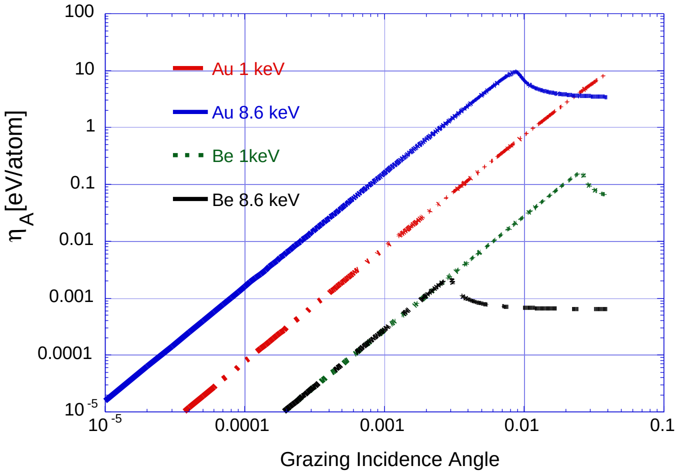

FIGURE 5. Energy loading of Au and Be vs. grazing incidence angle at photon energies of 1 and 8.6 keV. Irradiation with the unattenuated LCLS beam is assumed.

4. DISCUSSION

In recent years, a number of efforts have been made to extend Michelson interferometry toward the X-ray range. A basic goal is an instrument with a non-dispersive broadband response, which would not only allow the analysis of the temporal structures of both broad and narrow band sources, but would enable the systematic extension of Fourier Transform Spectroscopy (FTS) toward substantially shorter wavelengths (1,9). Without exception, the primary obstacle to realizing a fully flexible instrument has been the relatively limited capabilities of optics in the X-ray regime. For example, efforts based on crystal reflectors tend to be band-limited (10), while structures utilizing broad-band reflectors in compact geometries (6) can rapidly lose efficiency at decreasing wavelengths and can be susceptible to tolerance and surface-quality limitations in extreme grazing incidence geometries. Successful development of our proposed interferometer, an instrument of the latter type, will require careful attention to all these details. On the other hand, the extremely high per-pulse flux of the LCLS will to some extent compensate for the limited efficiency of the device at Å wavelengths. In this regard, a number of points relevant to the performance and operation of the proposed instrument can be made.

First, the practically attainable path length difference of the instrument is of the order of 20μ, at least for interferometer lengths of 2m or less. However, since the resolution is given by $\delta\nu/\nu \sim (\lambda/\Delta r)$, this still correponds to a resolution of the order of 5×10^{-6} at 8.5 keV. For larger values of θ_1 or substantially longer arm path lengths, correspondingly longer path length differences (and resolutions) could be generated. Second, as the path length difference is tuned, the detector need not record the detailed fringe pattern associated with a given pulse. A mask consisting of apertures smaller than $\sim \lambda/(8(\theta_1-\Delta\theta))$, and with a varying period equal to the varying fringe pattern period, followed by an intensity detector would be adequate, provided the contrast ratio of the interference pattern remains sufficiently high over the operating range of the instrument. A mask of this type could be fabricated as a variable-period multilayer consisting of alternating high-Z/low-Z materials and operated in transmission. Third, photon flux estimates indicate that a detector that *could* record the fringe pattern would also be feasible, even at 1.5 Å. This is based on two factors. The first is that at the small angles θ_1 of operation the wavelength of the interference pattern will be dilated by the factor $(2(\theta_1-\Delta\theta))^{-1}$. In practical terms, periods in the 50-1500 Å range are known to be recordable. The second point is that while recording materials that operate down to this level of resolution (e.g., PMMA, or Ag-doped semiconductors) are known to require large amounts of energy per unit area (O(1 J/cm^2)), such (single-shot) exposure requirements could easily be met by the LCLS, even far away from saturation.

Next, as regards the beam splitter, it is easily estimated that in order to attain a θ_1 in the >0.005 rad range at 1.5 Å, grating periods of 300 Å or less will be required. Such structures, similarly to the masks described above, could be fabricated as multilayers and operated in transmission, a technique that has been developed in recent years at LLNL (11,12). Blurring of the LCLS temporal structure due to the splitter's dispersive effects (5) could to a certain extent be mitigated by pinhole aperturing of the incoming light. Splitting methods based on homogeneous or perforated (6) foils operating in transmission/reflection could also be investigated, particularly if the practical performance of the grating splitter proves to be overly dispersion-limited. In this context, the development of broad-band, high-quality multilayers as alternatives to the specular reflectors assumed here could be pursued as a means of scaling down the length of the instrument, particularly for FTS or source-analysis applications for which the bandwidth reduction would be acceptable.

Finally, perhaps the most critical issue concerns the tolerances required on the alignments, positions, and motions of the interferometer components. In this regard, although an exhaustive discussion is outside the scope of this article, a number of points can be made. First, tolerance specifications will be determined to a large extent by the optical components utilized in the interferometer, the type of detector, and mode of operation of the instrument. For example, starting with the splitter, it is well-known that the far-field diffraction pattern of a normal-incidence transmission grating is invariant with respect to the transverse coordinates of the grating. Moreover, while it *is* sensitive to the inclination of the grating away from normal incidence, the dispersion angles vary with the cosine of the deviation angle, making the tolerance on the deviation of this parameter for controlling the lateral motion of the split beams to , say, the ~10^{-9} rad level fairly robust (~10-100 μrad). However the following elements, the mirrors, *will* require exceptionally stringent tolerances both on position and angle should, for example, maintenance of the interference pattern's lateral position on the detector plane to a fraction of the pattern's wavelength be required. This requirement would be necessary if operating with a mask followed by an intensity detector (as described above), and may well represent the limit on the lowest attainable wavelength that a practical device could operate at. However, these tolerances could be minimized if the detector was a resist that recorded the interference pattern of each shot. In this case the autocorrelation could be unfolded from the distribution and statistics of the interference pattern, and these would be substantially less sensitive to its lateral position. In the same context, it can be noted that the ability to control the interference patterns' lateral positions *could* be considerably enhanced - even for dispersion lengths of 1-2 meters - by replacing the mirrors with transmission grating splitters (the one corresponding to M1 being also rotatable), which would result in the same tolerance reduction as for the incoming beam splitter. Here again the copious flux of the LCLS would more than compensate for the substantially lower efficiency of the grating deflectors. Needless to say, the duration of the LCLS recording events will be so short that questions of tolerance on any component's motion *during* recording can be completely disregarded. In view of all these observations, the expectation is that tolerance issues will constitute perhaps the most challenging aspect of the development of the proposed interferometer, but that with successfully directed R&D - coupled with the unique source properties of the LCLS - configurations or modes of operation of the instrument can be identified for which the tolerance requirements will be manageable.

ACKNOWLEDGMENTS

This work was supported in part by the Department of Energy Offices of Basic Energy Sciences and High Energy and Nuclear Physics, and Department of Energy

Contract DE–AC03–76SF00515. Other portions of this work were supported by Department of Energy CRADA SLAC-9302.

REFERENCES

1. Fowles, G. R., *Introduction to Modern Optics*, New York: Holt, Rinehart and Winston, Inc., 1975, ch. 3, pp. 33-80.
2. Murphy, J. B., Pellegrini, C. "Introduction to the Physics of the Free Electron Laser," in *Frontiers of Particle Beams*, M. Month, S. Turner, eds., Lecture Notes in Physics No. 296, H. Araki et al, eds., Springer-Verlag, Berlin, 1988, pp. 163-212.
3. Tatchyn, R., Arthur, J., Boyce, R., Cremer, T., Fasso, A., Montgomery, J., Vylet, V., Walz, D., Yotam, R., Freund, A. K., Howells, M. R., "X-ray Optics Design Studies for the 1.5-15 Å Linac Coherent Light Source (LCLS) at the Stanford Linear Accelerator Center (SLAC)," SPIE Proceedings 3154, 174-222 (1998).
4. Tatchyn, R., Materlik, G., Freund, A., Arthur, J., eds., *Proceedings of the SLAC/DESY International Workshop on the Interactions of Intense Sub-Picosecond X-Ray Pulses with Matter*, SLAC, Stanford, CA, Jan. 23-24, 1997, SLAC WP-12.
5. Tatchyn, R., "Short-pulse limits in optical instrumentation design for the SLAC Linac Coherent Light Source (LCLS)," presented at the SRI'99 Conference, Stanford, CA, October 13-15, 1999; ms. #Wed--34, elsewhere these Proceedings..
6. Moler, E. J., Duarte, R. M., Howells, M. R., Hussain, Z., Oh, C., Spring, J., "First measurements using the ALS soft x-ray Fourier transform spectrometer," SPIE Proceedings 3154, 117-122 (1997).
7. Cremer, T., Tatchyn, R., "XREFLECTION: A New Graphical Database and Optics Simulation Utility at SSRL," in SSRL Newsletter, Fall 1996.
8 LCLS Design Study Group, Linac Coherent Light Source (LCLS) Design Study Report, SLAC-R-521, UC-414.
9. Bell, R. J., *Introductory Fourier Transform Spectroscopy*, New York: Academic Press, 1972.
10. Appel, A., Bonse, U., "Michelson Interferometer for X-Rays and Thermal Neutrons," Phys. Rev. Lett. 67(13), 1673-1676 (1991).
11. Bionta, R. M., Jankowski, A. F., Makowiecki, D. M., "Fabrication and Evaluation of Transmissive Multilayer Optics for 8 keV X Rays," Mat. Res. Soc. Symp. Proc. Vol. 103, 1993, pp. 257-263.
12. Bionta, R. M., "Transmission gratings that diffract 8 keV x rays," Appl. Phys. Lett. 51(10), 725-727 (1987).